How Can Ca^{2+} Selectively Activate Recoverin in the Presence of Mg^{2+}? Surface Plasmon Resonance and FT-IR Spectroscopic Studies†

Takeaki Ozawa,‡,§ Mami Fukuda,‡ Masayuki Nara,|| Akio Nakamura,⊥ Yoshiko Komine,‡ Kazuhiro Kohama,⊥ and Yoshio Umezawa*,‡,§

Department of Chemistry, School of Science, The University of Tokyo, Hongo, Bunkyo-ku, Tokyo 113-0033, Japan, Japan Science and Technology Corporation (JST), Tokyo, Japan, Laboratory of Chemistry, College of Liberal Arts and Sciences, Tokyo Medical and Dental University, Ichikawa, Chiba 272-0827, Japan, and Department of Pharmacology, School of Medicine, Gunma University, Maebashi, Gunma 371-5811, Japan

Received August 15, 2000; Revised Manuscript Received September 18, 2000

ABSTRACT: We investigated the relationship between metal ion selective conformational changes of recoverin and its metal-bound coordination structures. Recoverin is a 23 kDa heterogeneously myristoylated Ca^{2+}-binding protein that inhibits rhodopsin kinase. Upon accommodating two Ca^{2+} ions, recoverin extrudes a myristoyl group and associates with the lipid bilayer membrane, which was monitored by the surface plasmon resonance (SPR) technique. Large changes in SPR signals were observed for Sr^{2+}, Ba^{2+}, Cd^{2+}, and Mn^{2+} as well as Ca^{2+}, indicating that upon binding to these ions, recoverin underwent a large conformational change to extrude the myristoyl group, and thereby interacted with lipid membranes. In contrast, no SPR signal was induced by Mg^{2+}, confirming that even though it accommodates two Mg^{2+} ions, recoverin does not induce the large conformational change. To investigate the coordination structures of metal-bound Ca^{2+} binding sites, FT-IR studies were performed. The EF-hands, Ca^{2+}-binding regions each comprising 12 residues, arrange to coordinate Ca^{2+} with seven oxygen ligands, two of which are provided by a conserved bidentate Glu at the 12th relative position in the EF-hand. FT-IR analysis confirmed that Sr^{2+}, Ba^{2+}, Cd^{2+}, and Mn^{2+} were coordinated to COO^- of Glu by a bidentate state as well as Ca^{2+}, while coordination of COO^- with Mg^{2+} was a pseudobridging state with six-coordinate geometry. These SPR and FT-IR results taken together reveal that metal ions with seven-coordinate geometry in the EF-hands induce a large conformational change in recoverin so that it extrudes the myristoyl group, while metal ions with six-coordinate geometry in the EF-hands such as Mg^{2+} remain the myristoyl group sequestered in recoverin.

Calcium ion is known to be distributed in all mammalian cells. Changes in cytosolic Ca^{2+} concentration evoke a wide range of cellular responses (*1*, *2*). Intracellular Ca^{2+}-binding proteins are the key molecules for transducing Ca^{2+} signaling via enzymatic reactions or modulation of protein−protein interactions. Mg^{2+} is essential like Ca^{2+} in biological systems, with structural and catalytic functions (*3*). Mg^{2+} is the most abundant divalent metal ion in mammalian cells, with the cytosolic free concentration kept nearly constant at 0.5−2.0 mM. In contrast to that of Mg^{2+}, the concentration of Ca^{2+} in the cytosol is 10^{-7} M, 4 orders of magnitude lower than that of Mg^{2+}. The regulation of cellular activities by Ca^{2+} is achieved through transient increases in the cytosolic concentration from 10^{-7} M in a resting cell to 10^{-6}−10^{-5} M in an activated cell (*2*). Thus, Ca^{2+} is able to regulate functions of Ca^{2+}-binding proteins even in a 100−10000-fold excess of Mg^{2+}. Discrimination of the Ca^{2+}-binding protein against Mg^{2+} is achieved by taking advantage of the larger ionic radius of Ca^{2+} and, possibly, special arrangement of coordinating oxygen ligands; Ca^{2+} takes a less stringent coordination number of 6−8, as compared with that of Mg^{2+}, which has a strong preference for 6-fold coordination in an octahedral symmetry (*4*).

The Ca^{2+}-binding region is composed of 40 amino acid residues, which has a conserved helix−loop−helix motif called the EF-hand domain (*5*, *6*). The EF-hand loop comprises 12 residues, which are arranged to coordinate Ca^{2+} with pentagonal bipyramid symmetry, with seven ligands provided by five side chain carboxylate oxygens, one backbone carbonyl oxygen, and one water oxygen. Two of the side chain ligands are provided by a highly conserved bidentate Glu in the 12th and last loop position (Figure 1A). Upon accommodating Ca^{2+}, it changes its conformation from a relatively compact, "closed" conformation to an "open" conformation (Figure 1B), and thereby, hydrophobic residues that had hidden in the internal portion of Ca^{2+}-binding proteins are exposed by these EF-hand domains. The hydrophobic residues in the Ca^{2+}-binding proteins interact with their target proteins and control their activity in the cell.

The Mg^{2+} dissociation constants of the EF-hands are in the millimolar range, and therefore, the high cytosolic Mg^{2+}

† This work has been supported by CREST (Core Research for Evolutional Science and Technology) of JST and by grants to Y.U. from the Ministry of Education, Science and Culture, Japan.

* To whom correspondence should be addressed. Phone: +81-3-5841-4351. Fax: +81-3-5841-8349. E-mail: umezawa@chem.s.u-tokyo.ac.jp.

‡ The University of Tokyo.

§ Japan Science and Technology Corporation (JST).

|| Tokyo Medical and Dental University.

⊥ Gunma University.

10.1021/bi001930y CCC: $19.00
Published on Web 11/02/2000

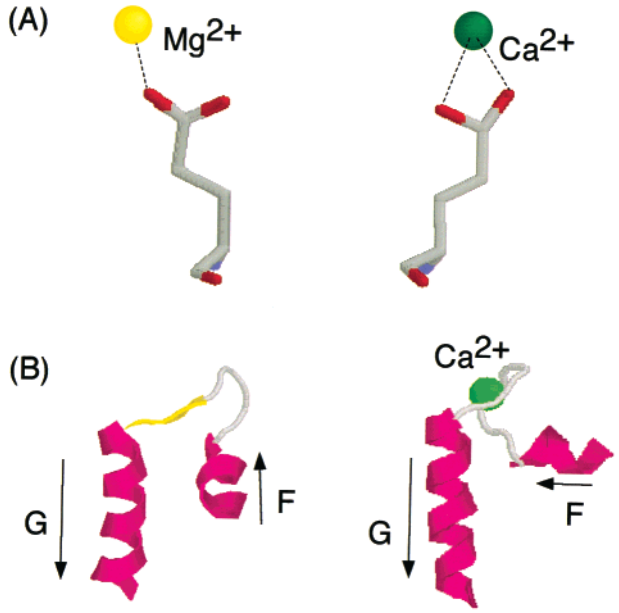

FIGURE 1: (A) Conformational transition of Glu in relative position 12 of an EF-hand binding site. This transition was described in the case of the EF-4 site of parvalbumin. (B) Three-dimensional structures of the closed ion-free (left) and open Ca^{2+}-loaded (right) states of EF-3 in recoverin. The backbone of the EF-hand loops is light gray; the β-sheet is yellow, and α-helices F and G are red. The Ca^{2+} ion is represented by a large green sphere. This figure was generated using Rasmol.

concentration implies that many EF-hands in the Ca^{2+}-binding protein are occupied by Mg^{2+} in resting cells. In contrast to those of Ca^{2+}, X-ray structures of Mg^{2+}-loaded EF-hand sites are only available for pike parvalbumin (*5*), myosin regulatory light chain (*6*), and calbindin D_{9k} (*7*). In parvalbumin and myosin regulatory light chain, the only difference between Mg^{2+} and Ca^{2+} ligation is that the residue in the 12th loop position serves as a monodentate ligand in the Mg^{2+} structures but as a bidentate ligand in the Ca^{2+} structures. In calbindin D_{9k}, the Glu in the 12th position is not used for direct Mg^{2+} ligation. Instead, a water molecule is inserted between the side chain and Mg^{2+}. The coordination geometry of the Glu in the 12th loop position has been shown to be very important for the structural rearrangements from a closed to an open conformation occurring upon Ca^{2+} binding (*8*−*15*).

Recoverin is one of the Ca^{2+}-binding proteins in retinal rod cells and serves as a Ca^{2+} sensor in vision (*16*, *17*). X-ray and NMR[1] studies on recoverin have shown that it has a compact globular shape of four EF-hands (*18*−*20*), which contrasts with the dumbbell shape of calmodulin (*21*−*24*) and troponin C (*25*). Only EF-2 and EF-3 of the four hands are capable of binding Ca^{2+} ions, whereas the remaining two sites of EF-1 and EF-4 do not have such an ability. EF-1 is distorted from a favorable Ca^{2+}-binding geometry by Cys-39 and Pro-40, and EF-4 contains a salt bridge between Lys-161 and Glu-171. The Ca^{2+}-loaded recoverin induces extrusion of a myristoyl group bound to the amino terminus and leads to its translocation from the cytosol to the lipid membranes (*26*, *27*).

[1] Abbreviations: SPR, surface plasmon resonance; FT-IR, Fourier transform infrared spectrometry; GST, glutathione *S*-transferase; ROS, rod photoreceptor outer segment; NMR, nuclear magnetic resonance.

To address the questions regarding how recoverin selectively transduces Ca^{2+} signals in the presence of the high concentration of cytosolic Mg^{2+} ions, we investigated metal ion selective conformational changes of recoverin and the coordination geometries of its metal ion-loaded EF-hand structures. To examine the interactions between metal ions and the side chain COO^- groups in the Ca^{2+}-binding sites of recoverin, the FT-IR method was used. The region of the COO^- antisymmetric stretch provides information about the modes of coordination of COO^- groups to the metal ions: bidentate, monodentate, or pseudobridging (*28*−*30*). To observe the conformational change of recoverin, selective association of recoverin to lipid membrane in the presence of Ca^{2+} or other possible interfering ions is monitored by the SPR technique (*28*). The obtained SPR and FT-IR results were used to conclude that bidentate ligation of COO^- of Glu in the 12th loop position of EF-hands to specific metal ions is a requisite for the global conformational changes in recoverin.

MATERIALS AND METHODS

Materials and Apparatus

Ethylenediamine-*N*,*N*,*N*′,*N*′-tetraacetic acid tetrasodium salt (EDTA), *O*,*O*′-bis(2-aminomethyl)ethylene glycol *N*,*N*,*N*′,*N*′-tetraacetic acid (EGTA), *N*-(2-hydroxyethyl)piperazine-*N*′-2-ethanesulfonic acid (HEPES), and 1-ethyl-3-(3-dimethylaminopropyl)carbodiimide hydrochloride (EDC) were obtained from Dojindo Laboratories (Kumamoto, Japan). Phosphatidylserine (PS), phosphatidylchorine (PC), and phosphatidylethanolamine (PE) were obtained from Sigma Chemical Co. (St. Louis, MO). 2-(2-Pyridinyldithio)-ethaneamine hydrochloride (PDEA) was obtained from BIAcore AB (Uppsala, Sweden). PreScission Protease was obtained from Amersham Pharmacia Biotech Inc. (Piscataway, NJ). Cadmium chloride ($CdCl_2$) was obtained from Kanto Chemical Co, Inc. (Tokyo, Japan). Deuterium oxide (D_2O) was obtained from Aldrich Chemical Co. (Milwaukee, WI). Other reagents were obtained from Wako Pure Chemical Ind. (Osaka, Japan) and were all of the highest purity available. All aqueous solutions were prepared with Milli-Q grade water (Millipore Reagent Water System, Millipore, Bedford, MA).

All SPR measurements were performed on a BIAcore-X system (Biacore AB, Uppsala, Sweden). A gold film called Sensor Chip CM5 (a carboxymethylated dextran attached to a gold-coated glass surface) was purchased from Pharmacia. Adjusting the pH of the buffer solutions was carried out with a glass electrode pH meter model HM-18E (TOA Electronics Co., Tokyo, Japan).

Methods

Sample Preparations of Recoverin. Myristoylated recoverin was purified from bovine retina extract using a phenyl-Sepharose affinity column and anion exchange chromatography (*28*). Unmyristoylated recoverin was extracted from *Escherichia coli* (DH5α) and purified. The transformed *E. coli* cells were cultured in LB ampicillin medium at 37 °C. Expression of GST recoverin was induced by addition of IPTG to a final concentration of 0.1 mM for 3 h at 37 °C. The cells were lysed in the buffer [150 mM NaCl, 1 mM

DTT, and 50 mM Tris-HCl (pH 7.5)] with a tip sonicator, and the solution was centrifuged at 10000*g* for 20 min at 4 °C. The supernatant obtained by the centrifugation was applied to a glutathione affinity column equilibrated with a washing buffer [150 mM NaCl, 1 mM DTT, and 50 mM Tris-HCl (pH 7.5)]. After the column had been washed with the same buffer, the adsorbed GST−recoverin fusion protein was cleaved in the column by injecting 80 units of PreScission Protease (Amersham Pharmacia Biotech Ltd., Chalfont, U.K.) and kept overnight. The cleaved recoverin was eluted with the washing buffer and dialyzed against Milli-Q water for 2 days to remove all salts. To further remove contaminated Ca^{2+}, 1 M $(NH_4)_2SO_4$ was added to an equilibration buffer containing 0.5 mM EGTA and 50 mM Tris-HCl (pH 7.5). The concentration of $(NH_4)_2SO_4$ decreased to 0.1 M. The obtained recoverin solution was applied to the Sephadex G-25 column to remove EGTA from recoverin. The purity of recoverin was evaluated by SDS−polyacrylamide gel electrophoresis with Coomassie Brilliant Blue staining. The purified recoverin gave a single band of 23 kDa. To exchange protons of recoverin with deuterium, recoverin was lyophilized and dissolved in D_2O, which was lyophilized again. Metal-bound recoverins were prepared by dissolving the powder of deuterated metal-free recoverin in a D_2O solution containing 50 mM Ca^{2+}, Mg^{2+}, Sr^{2+}, and Ba^{2+} or 5 mM Cd^{2+} and Mn^{2+} (pD 7.5).

Flow Dialysis. Ca^{2+}-binding curves in the presence of various concentrations of Mg^{2+} were obtained by the flow dialysis method using a home-built apparatus as described previously (*29*). The dialysis medium contained 0.1 mM unmyristoylated recoverin in 0.1 M NaCl and 20 mM MOPS/NaOH (pH 7.0) at 25 °C. The Ca^{2+}-binding data were quantitatively analyzed using the two-site equations.

FT-IR Assessments of Recoverin with Metal Ions. FT-IR spectra were recorded under a dry nitrogen atmosphere with a resolution of 2 cm^{-1} on a model 1720-X instrument (Perkin-Elmer, Norwalk, CT) in a room thermostated at 25 °C. A gap between the CaF_2 plates was sealed with aluminum tape to suppress the evaporation of water. About 10 μL of each sample solution was set between two CaF_2 plates using a 0.015 mm Teflon spacer. Well-resolved spectra for metal-free or -bound recoverin were obtained by subtracting the spectrum of a buffer solution from that of the corresponding protein solution (difference spectra); otherwise, the large background spectrum arising from D_2O would preclude interpretation of the spectrum from the protein of interest.

Preparation of Liposomes. A mixture of 4 mg of lipids [40% (w/w) PE, 40% (w/w) PC, 15% (w/w) PS, and 5% (w/w) cholesterol in $CHCl_3$], corresponding to the lipid composition in bovine ROS membranes (*30*), was dried in a vacuum with a speed vacuum concentrator, and the resulting phospholipid film was dried overnight using a vacuum pump to evaporate $CHCl_3$ completely. The film was resuspended in a buffer [150 mM KCl and 20 mM HEPES (pH 7.5)] and sonicated for 3 × 5 s. This suspension was preserved under nitrogen at 4 °C. The liposome solution was diluted with buffers consisting of each concentration of metal ion, 150 mM KCl, and 20 mM HEPES (pH 7.5). For the preparation of Ca^{2+}, Mg^{2+}, Sr^{2+}, and Ba^{2+} sample solutions, 0.5 mM EGTA was added to the metal buffer to mask contaminated Ca^{2+} ions. These metal solutions were filtered twice through a polycarbonate filter (pore size of 0.8 and 0.4 mm, Millipore Co.), which was used for the SPR measurements.

Measurements of SPR Signals. Recoverin was immobilized by a method for coupling proteins on a dextran matrix attached to a gold surface via thiol groups of cysteine (*28*, *31*). The recoverin-immobilized dextran matrix on the gold surface was equilibrated with a running buffer [0.5 mM EGTA, 150 mM KCl, and 10 mM HEPES (pH 7.5)]. The operating temperature for all SPR measurements was 25.0 °C. Ca^{2+} solutions were prepared, consisting of the liposome solution [0.5 mM EGTA, 150 mM KCl, 20 mM $MgCl_2$, and 10 mM HEPES (pH 7.5)] and each concentration of Ca^{2+}. The concentration of free Ca^{2+} in a given concentration of EGTA was determined by using the conditional formation constant for the Ca^{2+}−EGTA complex at pH 7.5, calculated from the formation constant for the Ca^{2+}−EGTA chelate (log $K = 11.0$, $I = 0.1$, 25 °C) and four acid dissociation constants for EGTA ($pK_1 \sim pK_4 = 2.08$, 2.73, 8.93, and 9.54, $I = 0.1$, 25 °C) (*32*). The samples were loaded into the injecting position of the SPR instrument. To remove all liposomes bound to immobilized recoverin, 0.5% Tween 20 dissolved in the running buffer was injected. This procedure was repeated at each concentration of free Ca^{2+}. In the cases of Mg^{2+}, Sr^{2+}, and Ba^{2+}, 0.5 mM EGTA was added into their sample solutions to mask contaminated Ca^{2+} from glass vessels. For Cd^{2+} and Mn^{2+}, the sample solutions were prepared in the absence of EGTA under otherwise identical conditions and were injected into the flow system. All the SPR measurements for each sample metal ion were repeated two or three times. The dextran matrix immobilizing recoverin had to be reproduced after the matrix was used for 1 week, because the magnitudes of the SPR signals decreased gradually even though the same sample solution was injected. The decrease in the magnitude of the SPR signals may originate from losing activity of recoverin and/or its dissociation from the dextran matrix. The amount of immobilized recoverin was not precisely controllable, which also affected changes in the absolute intensity of the SPR signals. Reproducibility of all the SPR measurements was therefore confirmed repetitively with different dextran matrixes, and representative data are shown in the figures.

RESULTS

Effect of Mg^{2+} on Ca^{2+} Binding to Unmyristoylated Recoverin

Ca^{2+} binding curves of unmyristoylated recoverin were determined by using the flow dialysis technique. Recoverin exhibits markedly biphasic Ca^{2+} binding, and the obtained curves appear to saturate at about two Ca^{2+} ions bound per recoverin (Figure 2), which was in good agreement with the one observed by the NMR studies in which two Ca^{2+} ions bind to recoverin. The Ca^{2+} binding curve was well-fitted by the two-site model as reported previously (*33*):

$$Y = \frac{(\beta_1^{app} + \beta_2^{app})x + 2\beta_1^{app}\beta_2^{app}x^2}{1 + (\beta_1^{app} + \beta_2^{app})x + \beta_1^{app}\beta_2^{app}x^2} \quad (1)$$

where Y is the fractional occupancy of the Ca^{2+}-binding sites of recoverin, β_1^{app} and β_2^{app} are the macroscopic association constants of the higher-affinity site (EF-3) and the lower-affinity site (EF-2), respectively, and x denotes the free Ca^{2+}

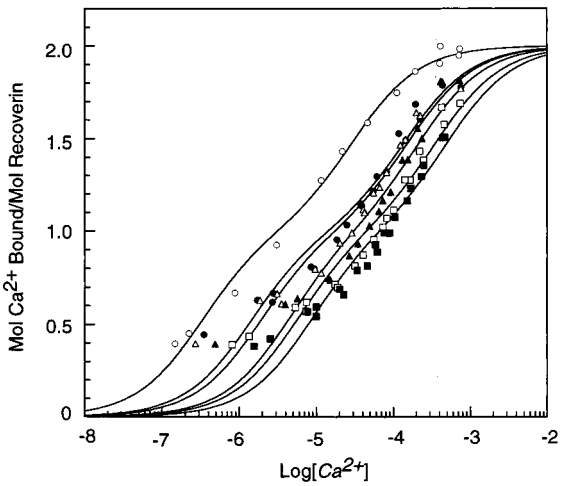

FIGURE 2: Ca^{2+} binding curves of unmyristoylated recoverin obtained by flow dialysis in the absence and presence of Mg^{2+}. The Mg^{2+} concentrations were as follows: 0 (○), 5 (●), 10 (△), 25 (▲), 50 (□), and 100 mM (■). The solid lines were drawn by using the two-site model, and the dissociation constants are listed in Table 1.

Table 1: Effects of Mg^{2+} on Macroscopic Association Constants Describing Ca^{2+} Binding to Recoverin

$[Mg^{2+}]$ (mM)	$1/\beta_1^{app}$ (mM)	$1/\beta_2^{app}$ (mM)
0	0.32	0.030
5	1.3	0.14
10	1.8	0.16
25	4.2	0.22
50	5.4	0.36[a]
100	8.3[a]	0.51[a]
	$1/\beta_1^{app}$ (mM)	$1/\beta_2^{app}$ (mM)
K_5 (M^{-1})	3.7×10^3	
K_{d1} (mM)[b]	2.7	
K_6 (M^{-1})		77
K_{d2} (mM)[b]		13
r^2	1.00	0.96

[a] These values were not used for the determination of Mg^{2+} binding constants. [b] $K_{d1} = 1/K_5$. $K_{d2} = 1/K_6$. All of the values in the column are dissociation constants.

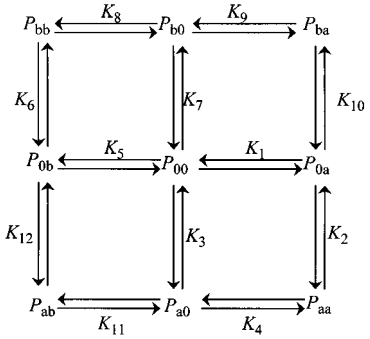

FIGURE 3: Two-site model for the binding of Ca^{2+} and Mg^{2+} to recoverin. The equilibrium expressions are defined in the text.

concentration. The obtained macroscopic association constants are shown in Table 1. The effects of Mg^{2+} on the macroscopic association constants characterizing the binding of Ca^{2+} are also shown in Figure 2 and Table 1. Mg^{2+} ion decreased the affinity of recoverin for Ca^{2+} even at concentrations as low as 5 mM.

The stepwise equilibrium model extended to the case of a protein capable of binding two different ligands on two sites can be adapted to quantitatively evaluate the association constants of Mg^{2+} for both sites (*34*). The binding equilibria for two different Ca^{2+}-binding sites in the presence of a given concentration of Mg^{2+} are depicted in Figure 3. The binding equilibria are

$$P_{00} + Ca^{2+} \leftrightarrow P_{0a} \quad \frac{P_{0a}}{P_{00}x} = K_1 \tag{2}$$

$$P_{0a} + Ca^{2+} \leftrightarrow P_{aa} \quad \frac{P_{aa}}{P_{0a}x} = K_2 \tag{3}$$

$$P_{00} + Ca^{2+} \leftrightarrow P_{a0} \quad \frac{P_{a0}}{P_{00}x} = K_3 \tag{4}$$

$$P_{a0} + Ca^{2+} \leftrightarrow P_{aa} \quad \frac{P_{aa}}{P_{a0}x} = K_4 \tag{5}$$

$$P_{00} + Mg^{2+} \leftrightarrow P_{0b} \quad \frac{P_{0b}}{P_{00}y} = K_5 \tag{6}$$

$$P_{0b} + Mg^{2+} \leftrightarrow P_{bb} \quad \frac{P_{bb}}{P_{0b}y} = K_6 \tag{7}$$

$$P_{00} + Mg^{2+} \leftrightarrow P_{b0} \quad \frac{P_{b0}}{P_{00}y} = K_7 \tag{8}$$

$$P_{b0} + Mg^{2+} \leftrightarrow P_{bb} \quad \frac{P_{bb}}{P_{b0}y} = K_8 \tag{9}$$

$$P_{b0} + Ca^{2+} \leftrightarrow P_{ba} \quad \frac{P_{ba}}{P_{b0}x} = K_9 \tag{10}$$

$$P_{0a} + Mg^{2+} \leftrightarrow P_{ba} \quad \frac{P_{ba}}{P_{0a}y} = K_{10} \tag{11}$$

$$P_{a0} + Mg^{2+} \leftrightarrow P_{ab} \quad \frac{P_{ab}}{P_{a0}y} = K_{11} \tag{12}$$

$$P_{0b} + Ca^{2+} \leftrightarrow P_{ab} \quad \frac{P_{ab}}{P_{0b}x} = K_{12} \tag{13}$$

where K_n is the association constant, P_{ij} denotes the occupancy of EF-hand sites i and j in recoverin, and x and y are the free Ca^{2+} and Mg^{2+} concentrations, respectively. Both sites are empty in P_{00}. Ca^{2+} is filled in P_{a0} and P_{0a}. Mg^{2+} is filled in P_{b0} and P_{0b}. Both sites are filled in P_{aa}, P_{bb}, P_{ab}, and P_{ba}. The fractional occupancy Y of the Ca^{2+}-binding sites is given by

$$Y = \frac{P_{0a} + P_{a0} + 2P_{aa} + P_{ba} + P_{ab}}{P_{00} + P_{0a} + P_{a0} + P_{aa} + P_{0b} + P_{b0} + P_{bb} + P_{ba} + P_{ab}} \tag{14}$$

If the two sites are independent of each other, i.e., the binding of Ca^{2+} to a specific site is not dramatically altered by the binding of Mg^{2+} to the other site, we obtain the following relationships:

$$K_1 = K_4 = K_9 \quad (15)$$

$$K_2 = K_3 = K_{12} \quad (16)$$

$$K_5 = K_8 = K_{11} \quad (17)$$

$$K_6 = K_7 = K_{10} \quad (18)$$

In this case, the fractional occupancy Y simplifies to

$$Y = \frac{(K_1 + K_2)x + 2K_1K_2x^2 + (K_1K_6 + K_2K_5)xy}{1 + (K_1 + K_2)x + K_1K_2x^2 + (K_5 + K_6)y + K_5K_6y^2 + (K_1K_6 + K_2K_5)xy} \quad (19)$$

Combining eqs 1 and 19, we derive the following relationships between the apparent macroscopic binding constants, experimentally determined, and the intrinsic binding constants of Ca^{2+} (K_1 and K_2) and Mg^{2+} (K_5 and K_6):

$$\frac{1}{\beta_1^{app}} = \frac{1}{K_1}(1 + K_5y) \quad (20)$$

$$\frac{1}{\beta_2^{app}} = \frac{1}{K_2}(1 + K_6y) \quad (21)$$

The data for the two Ca^{2+}-binding sites were fitted to eqs 20 and 21 (see ref *34* for a more general approach to the study of multiple ligands binding to a macromolecule). A linear regression analysis of the data gave values for K_5 and K_6, and the coefficient of correlation r^2 which permits an estimation of the fitness of the model used for calculating the binding constants. The values of K_5, K_6, and each coefficient of correlation r^2 are reported in Table 1. The competition experiments indicate that Ca^{2+}-binding sites bind Mg^{2+} competitively in a millimolar range.

Coordination Structures of Metal-Bound EF-Hands

A general trend has been found in the relationship between the type of coordination of the COO^- group to divalent metal cations and the position of the antisymmetric stretch of the COO^- group [$\nu_{as}(COO^-)$] by examining data observed for the acetate anion (*35*). These general trends were summarized as follows. (I) Bidentate coordination of the COO^- group to a divalent metal cation downshifts the position of the $\nu_{as}(COO^-)$ band from that of the free COO^- group that is not interacting with a metal cation. (II) Unidentate coordination of the COO^- group to a divalent metal cation upshifts the $\nu_{as}(COO^-)$ band from the position of the $\nu_{as}(COO^-)$ band, which is not interacting with metal ions. (III) In the pseudobridging coordination where one divalent metal cation is bound to either of the two oxygens in the COO^- group and a water molecule is hydrogen-bonded to the other oxygen, the position of the $\nu_{as}(COO^-)$ band is close to that of the free $\nu_{as}(COO^-)$ band. These empirically determined rules were supported by ab initio molecular orbital (MO) calculations (*36*) and have been applied to examine interactions between COO^- groups in the Ca^{2+}-binding protein and metal cations (*37*, *38*). To elucidate the coordination geometries of the metal-bound EF-hands in recoverin, we studied the infrared spectra from the antisymmetric stretch of the COO^- stretch in recoverin.

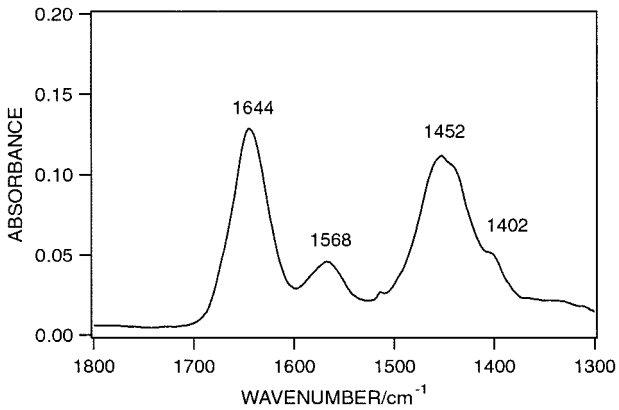

FIGURE 4: Infrared spectra (1800−1300 cm^{-1}) of the metal-free forms of recoverin in D_2O.

The infrared spectrum (1800−1300 cm^{-1}) of metal-free recoverin in D_2O solution is shown in Figure 4, where absorptions of D_2O have already been subtracted. Four broad bands were observed: the amide I′ band at 1644 cm^{-1}, the COO^- antisymmetric stretching band at 1568 cm^{-1}, the amide II′ band at 1452 cm^{-1}, and the COO^- symmetric stretching band at 1402 cm^{-1}. Because the infrared spectra of metal ion-bound recoverin exhibited patterns very similar to those of metal-free recoverin for Ca^{2+}, Mg^{2+}, Sr^{2+}, Ba^{2+}, Cd^{2+}, or Mn^{2+}, it was difficult to distinguish between the metal-free and metal-bound forms. We obtained the second-derivative spectra to more accurately detect the difference (Figure 5).

When the second-derivative spectrum of the Ca^{2+}-bound form was compared with that of the metal-free form, clear differences were found in the region of the COO^- antisymmetric stretch. The metal-free form has only two bands, 1584 and 1566 cm^{-1} (Figure 5a). In contrast with the metal-free form, another band at 1544 cm^{-1} in the Ca^{2+}-bound form was observed in addition to the two bands (Figure 5b). The intensity of the band at 1566 cm^{-1} of the Ca^{2+}-bound form seems to be lower than that of the corresponding band of the metal-free form, indicating that the band at 1544 cm^{-1} was downshifted from 1566 cm^{-1}.

The 1544 cm^{-1} band, downshifted 22 cm^{-1} from the 1566 cm^{-1} band, was consistent with the general trend experimentally found and with the MO studies; the band at 1544 cm^{-1} of the Ca^{2+}-bound form is undoubtedly due to the COO^- groups of Glu at the last position of the EF-hand loops, which are coordinated to Ca^{2+} in the bidentate mode. This bidentate coordination of Ca^{2+}-bound EF-hands has also been revealed by X-ray analysis, in which the COO^- groups of Glu-85 and Glu-121 were bidentate in the Ca^{2+}-bound form (*19*). It is therefore concluded that Ca^{2+} coordinates COO^- of the Glu in the bidentate state and takes as a whole seven-coordinate geometry in the EF-hand domains.

The spectra of the Sr^{2+}-, Ba^{2+}-, and Mn^{2+}-bound forms have features in common with those of the Ca^{2+}-bound forms. There are three peaks at 1584, 1564, and 1544 cm^{-1} in the region of $\nu_{as}(COO^-)$ of the metal-bound form. The peak at 1544 cm^{-1} was downshifted from the 1566 cm^{-1} band of the metal-free from, indicating that these metal ions have bidentate coordination like the Ca^{2+}-bound form. The Cd^{2+}-bound form also has three bands at 1584, 1564, and 1544 cm^{-1} as observed in the Ca^{2+} case. However, the

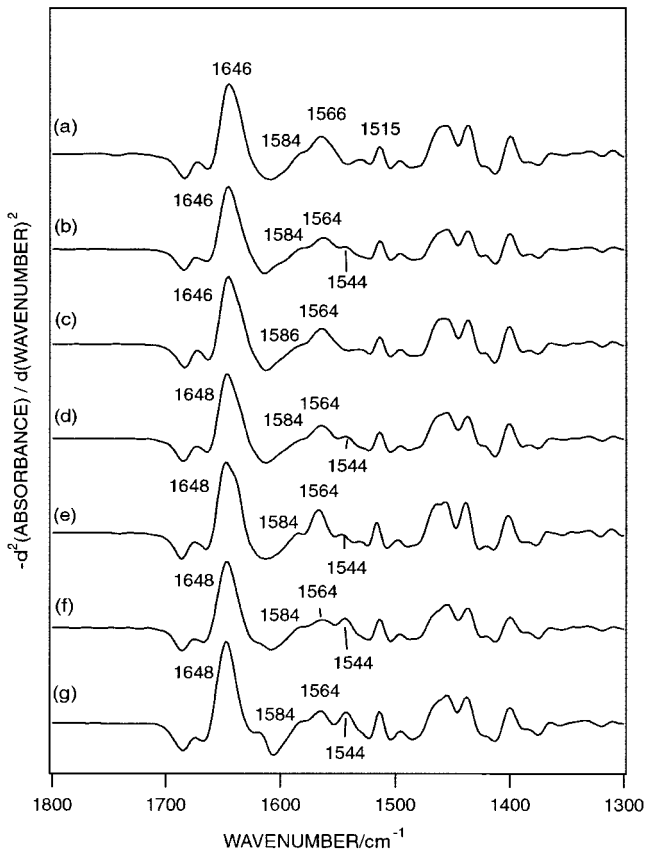

FIGURE 5: Infrared second-derivative spectra (1800−1300 cm^{-1}) of the metal-free and metal-bound forms of recoverin in D_2O solution: (a) metal-free form, (b) Ca^{2+}-bound form, (c) Mg^{2+}-bound form, (d) Sr^{2+}-bound form, (e) Ba^{2+}-bound form, (f) Cd^{2+}-bound form, and (g) Mn^{2+}-bound form.

spectral pattern in this region of $\nu_{as}(COO^-)$ of the Cd^{2+}-bound form was different from that of the Ca^{2+}-bound form. The intensity of the 1564 cm^{-1} peak of the Cd^{2+}-bound form was lower than that of the Ca^{2+}-bound form, and the intensity of the 1544 cm^{-1} peak of the Cd^{2+}-bound form was higher than that of the Ca^{2+}-bound form. This phenomena may be due to the fact that Cd^{2+} also binds to other COO^- groups in addition to the one in the EF-hands. To verify that a peak at 1544 cm^{-1} is from $\nu_{as}(COO^-)$ of Glu, subtraction of the spectrum of the Cd^{2+}-bound form from that of the metal-free form was performed. The obtained spectrum showed that the peak at 1544 cm^{-1} was enhanced and the magnitude of the peak at 1564 cm^{-1} was reduced (data not shown), indicating that the peak at 1544 cm^{-1} in the Cd^{2+}-bound form downshifted from the 1566 cm^{-1} band of the metal-free form. To prove that Cd^{2+} ions bind to other COO^- groups in addition to Glu in the EF-hands, the spectra of the Cd^{2+}-bound form at five different Cd^{2+} concentrations (1, 2, 3, 4, and 5 mM) have been measured. Figure 6 shows the dependence of the spectra on each Cd^{2+} concentration. No fluctuation in the recoverin concentration is validated from a constant peak intensity at 1515 cm^{-1}, which was assinged to be a C−C stretch of aryl groups of tyrosine. When the Cd^{2+} concentration was increased, the peak intensity at 1544 cm^{-1} increased, while the intensity at 1564 cm^{-1} decreased. Because the recoverin concentration is ∼2 mM and there are two metal-binding sites in recoverin, two metal-binding sites of recoverin are occupied by Cd^{2+} at a concentration as high as 4 mM. In Figure 6d (the concentration of Cd^{2+} is

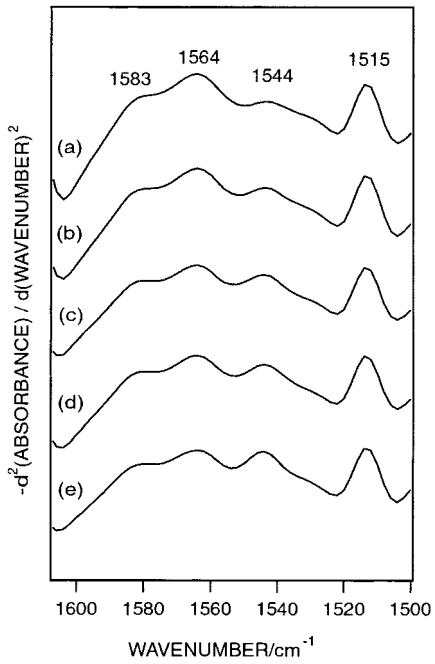

FIGURE 6: Cd^{2+} concentration dependence on infrared second-derivative spectra (1600−1500 cm^{-1}) of recoverin: (a) 1, (b) 2, (c) 3, (d) 4, and (e) 5 mM.

4 mM), the peak intensities in the region of $\nu_{as}(COO^-)$ were similar to that of the Ca^{2+}-bound form, indicating that Cd^{2+} specifically binds to the EF-hands. When the fact that the peak intensity at 1544 cm^{-1} in the case of 5 mM Cd^{2+} (Figure 6e) was enhanced more than that of 4 mM Cd^{2+} is considered, it is concluded that the excess Cd^{2+} ions bind Glu of the other part of recoverin.

In contrast to the metal ions described above, the spectrum of the Mg^{2+}-bound form has only two bands in the region of $\nu_{as}(COO^-)$: 1586 cm^{-1} from aspartic acids and 1564 cm^{-1} from glutamic acids. There is no peak at 1544 cm^{-1}. The spectral pattern of the Mg^{2+}-bound form is closer to that of the metal-free form, indicating that Mg^{2+} binds to recoverin with unidentate (pseudobridging) coordination or the Mg^{2+}-unoccupied form in the EF-hands.

Conformational Changes in Recoverin

(1) Response for Ca^{2+}. When recoverin was immobilized on the dextran matrix and a Ca^{2+} sample solution containing liposomes was injected, association of the recoverin−Ca^{2+} complex with the liposome was revealed as a response of the SPR signal. A typical time profile of the SPR signal with a Ca^{2+} concentration of 1×10^{-3} M is shown in Figure 7A. An initial baseline for the SPR signal after conditioning the sensing membrane in a running buffer was defined as 0 RU. With injection of sample solutions containing 1×10^{-3} M Ca^{2+}, an increase in the magnitudes of the SPR signals was observed for 4 min, indicating that recoverin induced its conformational change on the dextran matrix by accommodating two Ca^{2+} ions and extruded its myristoyl group, allowing recoverin to interact with liposomes. When the sample solution was changed to the running buffer, the magnitudes of the SPR signals abruptly decreased. Complete dissociation of liposomes bound to the immobilized recoverin was achieved by injecting 0.5% Tween 20 dissolved in the running buffer, and the SPR signals returned to the baseline.

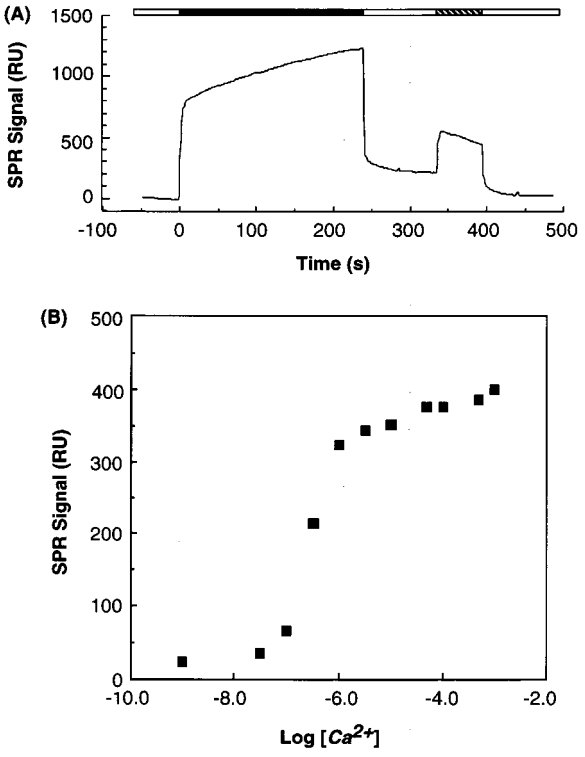

FIGURE 7: (A) Typical time profile of the SPR signal. A liposome solution containing 1.0×10^{-3} M Ca^{2+} was passed through the recoverin-immobilized gold surface (horizontal closed bar). To regenerate the gold surface completely, 0.5% Tween 20 flowed for 2 min (hatched bar). Injections of a running buffer containing 0.5 mM EGTA, 150 mM KCl, and 10 mM HEPES/NaOH (pH 7.5) were performed to equilibrate the sensor surface (white bar). (B) Dependence of the observed SPR signals on the concentrations of free calcium ions. Each data point was taken from the SPR signals (Figure 7) observed 4 min after the injection of Ca^{2+} sample solutions. The Ca^{2+} concentrations were calculated on the basis of the respective conditional stability constants for the 1:1 metal ion−EGTA complex.

The maximal amplitude of ~1200 RU at the end of injection of the Ca^{2+} sample solution originated from binding of liposomes to the immobilized recoverin and a large change in the bulk refractive index caused by the high concentrations of Ca^{2+} solutions. The change in the bulk refractive index was estimated to be ~800 RU by injecting the sample solution over the gold surface in the absence of recoverin (data not shown). To offset this background and yield net signals, the SPR signal measured for each sample solution in the presence of recoverin was corrected for the one in the absence of recoverin under otherwise identical conditions.

Figure 7B shows the dependence of the magnitudes of the observed SPR signals on the concentration of free calcium ions. To determine Ca^{2+}-relevant SPR signals, the Ca^{2+}-dependent signals, which were defined as the offset SPR signals obtained at 240 s, were evaluated as the difference in SPR signals between those for the running buffer solution and for the Ca^{2+} sample solution. With increasing concentrations of Ca^{2+} (from 1.1×10^{-7} to 1.5×10^{-6} M), the magnitude of the SPR signal sharply increased. A further increase in Ca^{2+} concentration did not yield any significant change in the SPR signals. The median effective value, ED_{50}, defined as the metal ion concentration yielding a half-maximum SPR signal (200 RU), was 4×10^{-7} M.

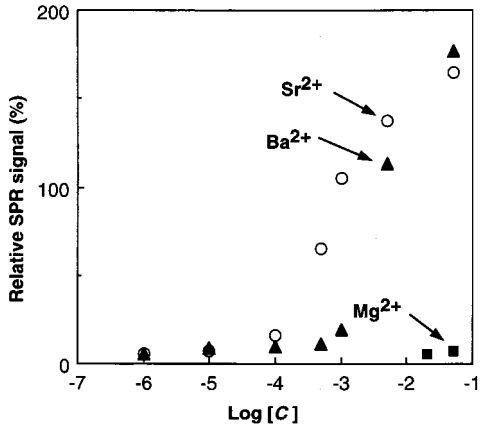

FIGURE 8: Dependence of the SPR signals on the concentrations of Sr^{2+}, Ba^{2+}, and Mg^{2+}.

(2) Responses to Mg^{2+}, Sr^{2+}, and Ba^{2+}. Time-dependent SPR signals in the association of liposomes with recoverin in the presence of Sr^{2+} and Ba^{2+} were similar to those for Ca^{2+}, while the ones for Mg^{2+} were silent (data not shown). The SPR signals obtained upon injection of sample solutions together with each concentration of Sr^{2+}, Ba^{2+}, or Mg^{2+} are shown in Figure 8. The *y*-axis represents the SPR signals (R) normalized according to the equation $R = 100(R_{metal}/R_{max})$, where R_{metal} is the magnitude of the SPR signals observed for those metal ions and R_{max} is the one for 1.0×10^{-3} M Ca^{2+}. A large increase in the magnitude of the SPR signal was observed with increasing concentrations of Sr^{2+} (from 1.0×10^{-4} to 1.0×10^{-3} M), and a moderate increase followed up to 1.0×10^{-2} M Sr^{2+}. At $<1.0 \times 10^{-4}$ M Sr^{2+}, no change in the SPR signals was observed. Ba^{2+} also induced an increase in the magnitude of the SPR signal from 5.0×10^{-3} to 1.0×10^{-2} M. The maximum response of the SPR signals for Sr^{2+} and Ba^{2+} was more than 100%, which was probably due to aggregation or fusion of liposomes. Liposomes are well-known to fuse or aggregate with high concentrations of alkaline earth metal ions (*40*). Responses for Sr^{2+} and Ba^{2+} indicate that both ions induce a conformational change in recoverin and are a substitute for Ca^{2+} in the concentration range that was examined. In contrast to the results for Sr^{2+} and Ba^{2+}, no change in the SPR signals was observed with Mg^{2+} even at concentrations of $\leq 5.0 \times 10^{-2}$ M, indicating that Mg^{2+} does not induce the extrusion of the myristoyl group of recoverin.

(3) Response to Cd^{2+} and Mn^{2+}. The sensorgram of the SPR signals for Cd^{2+} or Mn^{2+} was similar to the one for Ca^{2+}, and the results of the SPR signals for Cd^{2+} and Mn^{2+}, obtained 240 s after injection of the sample solution, are shown in Figure 9. With an increase in the Cd^{2+} concentration from 1.0×10^{-5} to 5.0×10^{-4} M, large increases in the magnitudes of the SPR signals were observed. Further increases in the concentration above 5.0×10^{-4} M decreased the magnitudes of the SPR signals. The initial increase in the magnitude of the SPR signals with increasing Cd^{2+} concentrations indicates that Cd^{2+} induced the conformational change in recoverin so that it interacts with the liposomes via the myristoyl group. The decreases in the magnitudes of the SPR signals following its maximum may be due to an allosteric feedback regulation of recoverin by excess Cd^{2+} ions. The magnitudes of the SPR signals for Mn^{2+} increased with its concentration from 1.0×10^{-5} to 5.0×10^{-3} M. At

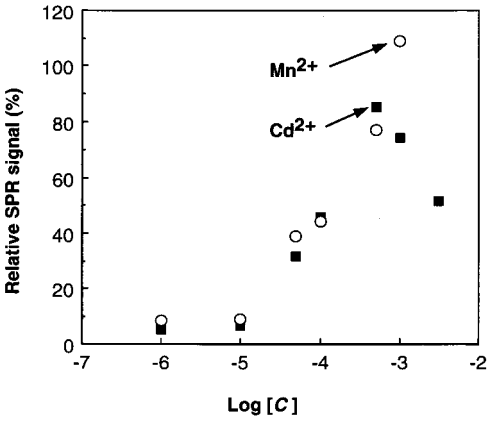

FIGURE 9: Dependence of the SPR signals on the concentrations of Cd^{2+} and Mn^{2+}.

$<1.0 \times 10^{-5}$ M Mn^{2+}, no SPR signal was observed. The responses for Mn^{2+} indicate that Mn^{2+} caused extrusion of the myristoyl group of recoverin so that it interacts with liposomes in the concentration range that was examined.

DISCUSSION

In the vertebrate photoreceptor cells, recoverin provides a Ca^{2+}-dependent feedback system involved in light adaptation by binding Ca^{2+} in the dark, when Ca^{2+} levels are high, and by releasing Ca^{2+} after its levels drop upon illumination. In the illuminated cells, Ca^{2+}-free recoverin should partially be bound with Mg^{2+} due to the existence of a millimolar Mg^{2+} concentration. It is therefore important to characterize the Mg^{2+} binding properties of recoverin to understand the reason Mg^{2+} binding does not exhibit an effect on the conformation of the protein similar to that of Ca^{2+}. Such knowledge will also shed light on the mechanism of the specific response of recoverin toward a narrow concentration fluctuation of Ca^{2+} in the presence of high levels of Mg^{2+}.

In the study presented here, coordination geometries of metal ions in the EF-hands of recoverin were determined by FT-IR studies to supplement SPR results for understanding how Ca^{2+} selectively activates intracellular signal transductions in the presence of a much higher cytosolic Mg^{2+} concentration. Clear differences between the coordination structures of Mg^{2+} and the other divalent metal ions that were examined are evident. Coordination of Ca^{2+}, Sr^{2+}, Ba^{2+}, Cd^{2+}, and Mn^{2+} to the COO^- group of Glu in the 12th position of EF-hands was bidentate; that is, these cations were seven-coordinate with the EF-hands in recoverin. In contrast, FT-IR spectra for Mg^{2+} could not unequivocally determine whether the coordination structure of Mg^{2+} to COO^- was the pseudobridging state or metal free. The flow dialysis analysis for evaluating the Mg^{2+} binding constants for each EF-hand in recoverin, however, concluded that both EF-hands were occupied with Mg^{2+} at 50 mM Mg^{2+}, and therefore, Mg^{2+} took a pseudobridging state and as a whole six-coordinate geometry with the EF hands in recoverin. SPR experiments carried out in the study presented here revealed that the seven-coordinate metal ions such as Ca^{2+}, Sr^{2+}, Ba^{2+}, Cd^{2+}, and Mn^{2+} induced extrusion of the myristoyl group of recoverin so it interacts with liposomes, whereas Mg^{2+}-bound recoverin, the coordination of which was a pseudobridging state, had its myristoyl group sequestered.

The fact that the Glu residue at relative position 12 and the last position in the cation-binding loops of the EF-hand proteins operates as an essential residue in $Ca^{2+}-Mg^{2+}$ exchange through its ability to switch between different conformational states has been studied extensively (*8*−*15*). Declercq et al. first demonstrated this in a study of a set of high-resolution crystal structures of pike muscle parvalbumin with their EF-hand sites occupied by Ca^{2+}, Mg^{2+}, or Mn^{2+}. Some remarkable, although subtle, changes in the parvalbumin conformation are associated with the substitution of Ca^{2+} with other divalent cations with different ionic radii, in one or both of the EF-hand cation-binding sites (see Figure 1) (*5*). This crystallographic study led to the discovery that the simple rotation of the Glu-101 (in EF-4) side chain site around its $C^{\alpha}-C^{\beta}$ bond allows a change in the coordination number of the central cation and the glutamyl residue, and thereby contributes as a bidentate ligand for Ca^{2+} and as a monodentate ligand for Mg^{2+}. In the EF-3 site of parvalbumin, the homologous glutamyl residue Glu-62 displays a behavior similar to that of Glu-101 upon $Ca^{2+}-Mg^{2+}$ exchange, based on NMR evidence (*41*) and, as suggested by an infrared study (*37*), as far as the switch between the bidentate and monodentate configurations is concerned. On the basis of the high-resolution crystal structure of the parvalbumin, Allouche et al. undertook a theoretical study using the free energy perturbation (FEP) method (*13*). The FEP calculation predicted the topology of the fully Mg^{2+}-loaded form for which no crystallographic data are presently available such as troponin C and calmodulin, in which the hexacoordination of Mg^{2+} corresponds with a regular octahedral configuration of the six oxygen atoms.

The coordination geometries of calmodulin and some other calcium binding proteins have been studied by the FT-IR method (*37*, *38*), by which the Glu in the 12th position in the Mg^{2+}-bound form of calmodulin was found to be a pseudobridging state and switched from the monodentate to the bidentate configuration when Mg^{2+} was substituted by Ca^{2+}. To better understand the Mg^{2+}-loaded calmodulin, NMR studies have been reported (*15*). When EF-hand structures of CaM change to their open conformation upon binding of Ca^{2+} ions, the CaM−metal complexes bind to M13, while if the EF-hand domains remain in their closed conformation even though Mg^{2+} binds, no CaM−Mg^{2+}−M13 complex is formed. When these FT-IR and NMR studies are considered, it is evident that Mg^{2+}-bound EF-hands of CaM were not of the open but closed conformation like the metal-free form because of its six-coordinate geometry with the EF-hands; the Mg^{2+}-loaded calmodulin does not undergo its conformational changes or interact with its targets. It is noteworthy that the correlation between the metal-bound coordination structures of calmodulin and the conformational change in calmodulin has been confirmed with other divalent cations. We have previously shown that coordination structures of Sr^{2+} and Cd^{2+} to COO^- as well as Ca^{2+} were bidentate in nature (*38*), and these metal ions induced a large conformational change from a dumbbell shape to a globular one for interaction with its target protein (*39*, *42*). On the contrary, the coordination structure of Mn^{2+} was unidentate like Mg^{2+}, and Mn^{2+}-loaded calmodulin did not bind to its target.

The conformational changes in the EF-hands in recoverin have been elucidated by X-ray and NMR (*18*−*20*). EF-3 of

the two EF-hands adopts an open conformation akin to that of the Ca^{2+}-occupied EF-hands in calmodulin and troponin C. The transition from the closed to open conformation of EF-3 in recoverin exposes hydrophobic residues, leading to a rotation of 45° of the N-terminal domain with respect to the other C-terminal domain, thereby promoting ejection of the myristoyl group. Since neither X-ray structures nor NMR data of Mg^{2+}-loaded EF-hand sites were available for recoverin at the time of this study, the structural rearrangements of the EF-hands remain unclear. However, when the NMR analysis of the structural change in recoverin together with those of the closed conformation of Mg^{2+}-loaded EF-hands for pike parvalbumin and for myosin regulatory light chain is taken into consideration, the present data for Mg^{2+} from flow dialysis, SPR, and FT-IR suggest that in the resting cell, EF-hands of recoverin are partially occupied with Mg^{2+}. The structure of Mg^{2+}-loaded EF-hands takes hexacoordination with a regular octahedral configuration of the six oxygen atoms and a closed conformation, which as a result remains the myristoyl group sequestered in recoverin.

In conclusion, we verified the relationship between the conformational change of recoverin induced by binding of metal ions and the coordination structures of metal-bound recoverin using the SPR technique and FT-IR spectroscopy. Metal ions such as Ca^{2+}, Sr^{2+}, Ba^{2+}, Cd^{2+}, and Mn^{2+}, which bind to the EF-hands of recoverin with seven-coordinate structures, i.e., bidentate coordination to COO^- of Glu in the EF-hand, induce conformational change in recoverin so it interacts with liposomes. On the other hand, Mg^{2+}-loaded EF-hand domains of recoverin have six-coordinate structure, that is, unidentate coordination to COO^- of Glu in the EF-hand, and remain the myristoyl group that is sequestered. In the resting state of eukaryotic cells, Mg^{2+} binds to the Ca^{2+}-binding loop of EF-hands to some extent, but the overall conformation is closed as for the ion-free recoverin, since the smaller Mg^{2+} does not allow the side chain carboxylates of the Glu in the 12th loop position into the coordination sphere. Our results support the hypothesis that the Glu residue at the 12th position of the EF-hand operates as an essential residue in $Ca^{2+}-Mg^{2+}$ exchange; the coordination requirement of one of the two physiologically relevant ions, Ca^{2+}, can be met upon binding to the protein with major rearrangement of the conformation, while Mg^{2+} ion, on the contrary, cannot fulfill this requirement.

REFERENCES

1. Shuttleworth, T. J. (1997) *J. Exp. Biol. 200*, 303−314.
2. Niki, I., Yokokura, H., Sudo, T., Kato, M., and Hidaka, H. (1996) *J. Biochem. 120*, 685−698.
3. Vogal, H. J. (1994) *Biochem. Cell Biol. 72*, 357−376.
4. Poonia, N. S., and Bajaj, A. V. (1979) *Chem. Rev. 79*, 389−445.
5. Declercq, J.-P., Tinant, B., Parello, J., and Rambaud, J. (1991) *J. Mol. Biol. 220*, 1017−1039.
6. Houdusse, A., and Cohen, C. (1996) *Structure 4*, 21−32.
7. Andersson, M., Malmendal, A., Linse, S., Ivarsson, I., Forsén, S., and Svensson, L. A. (1997) *Protein Sci. 6*, 1139−1147.
8. Malmendal, A., Evenäs, J., Thulin, E., Gippert, G. P., Drakenberg, T., and Forsén, S. (1998) *J. Biol. Chem. 273*, 28994−29001.
9. Evenäs, J., Thulin, E., Malmendal, A., Forsén, S., and Carlström, G. (1997) *Biochemistry 36*, 3448−3457.
10. Evenäs, J., Malmendal, A., Thulin, E., Carlström, G., and Forén, S. (1998) *Biochemistry 37*, 13744−13754.
11. Evenäs, J., Forsén, S., Malmendal, A., and Akke, M. (1999) *J. Mol. Biol. 289*, 603−617.
12. Gagné, S. M., Li, M. X., and Sykes, B. D. (1997) *Biochemistry 36*, 4386−4392.
13. Allouche, D., Parello, J., and Sanejouand, Y.-H. (1999) *J. Mol. Biol. 285*, 857−873.
14. Malmendal, A., Linse, S., Evenäs, J., Forsén, S., and Drankenberg, T. (1999) *Biochemistry 38*, 11844−11850.
15. Ohki, S., Ikura, M., and Zhang, M. (1997) *Biochemistry 36*, 4309−4316.
16. Dizhoor, A. M., Ray, S., Kumar, S., Niemi, G., Spencer, M., Brolley, D., Walsh, K. A., Philipov, P. P., Hurley, J. B., and Stryer, L. (1991) *Science 251*, 915−918.
17. Lambrecht, H. G., and Koch, K. W. (1991) *EMBO J. 10*, 793−798.
18. Tanaka, T., Ames, J. B., Harvey, T. S., Stryer, L., and Ikura, M. (1995) *Nature 376*, 444−447.
19. Flaherty, K. M., Zozulya, S., Stryer, L., and Mckay, D. B. (1993) *Cell 75*, 709−715.
20. Ames, J. B., Ishima, R., Tanaka, T., Gordon, J. I., Stryer, L., and Ikura, M. (1997) *Nature 389*, 198−202.
21. Chattopadhyaya, R., Meador, W. E., Means, A. R., and Quincho, F. A. (1992) *J. Mol. Biol. 228*, 1177−1192.
22. Babu, Y. S., Bugg, C. E., and Cook, W. J. (1988) *J. Mol. Biol. 204*, 191−204.
23. Zhang, M., Tanaka, T., and Ikura, M. (1995) *Nat. Struct. Biol. 2*, 758−767.
24. Kuboniwa, H., Tjandra, N., Grzesiek, S., Ren, H., Klee, C. B., and Bax, A. (1995) *Nat. Struct. Biol. 2*, 768−776.
25. Herzberg, O., and James, M. N. G. (1988) *J. Mol. Biol. 203*, 761−779.
26. Zozulya, S., and Stryer, L. (1992) *Proc. Natl. Acad. Sci. U.S.A. 89*, 11569−11573.
27. Dizhoor, A. M., Chen, C. K., Olshevskaya, E., Sinelnikova, V. V., Phillipov, P., and Hurley, J. B. (1993) *Science 259*, 829−832.
28. Lange, C., and Koch, K.-W. (1997) *Biochemistry 36*, 12019−12026.
29. Nakashima, K., Maekawa, H., and Yazawa, M. (1996) *Biochemistry 35*, 5602−5610.
30. Anderson, R. E., and Maude, M. B. (1970) *Biochemistry 9*, 3624−3628.
31. Satpaev, D. K., Chen, C.-K., Scotti, A., Simon, M. I., Hurley, J. B., and Slepak, V. Z. (1998) *Biochemistry 37*, 10256−10262.
32. Sillén, L. G., and Martell, A. E. (1964) *Stability Constants Supplement No. 1*, The Alden Press, Oxford, U.K.
33. Ames, J. B., Porumb, T., Tanaka, T., Ikura, M., and Stryer, L. (1995) *J. Biol. Chem. 270*, 4526−4533.
34. Haiech, J., Klee, C. B., and Demaille, J. G. (1981) *Biochemistry 20*, 3890−3897.
35. Deacon, G. B., and Phillips, R. J. (1980) *Coord. Chem. Rev. 33*, 227−250.
36. Nara, M., Torii, H., and Tasumi, M. (1996) *J. Phys. Chem. 100*, 19812−19817.
37. Nara, M., Tasumi, M., Tanokura, M., Hiraoki, T., Yazawa, M., and Tsutsumi, K. (1994) *FEBS Lett. 349*, 84−88.
38. Nara, M., Tanokura, M., Yamamoto, T., and Tasumi, M. (1995) *Biospectroscopy 1*, 47−54.
39. Ozawa, T., Sasaki, K., and Umezawa, Y. (1999) *Biochim. Biophys. Acta 1434*, 211−220.
40. Oku, N., and MacDonald, R. C. (1983) *Biochemistry 22*, 855−863.
41. Blancuzzi, Y., Padilla, A., Cave, A., and Parello, J. (1993) *Biochemistry 32*, 1302−1309.
42. Ozawa, T., Kakuta, M., Sugawara, M., and Umezawa, Y. (1997) *Anal. Chem. 69*, 3081−3085.

BI001930Y